International Journal of Occupational Safety and Ergonomics

ISSN: (Print) (Online) Journal homepage: www.tandfonline.com/journals/tose20

Three-dimensional heat and moisture transfer analysis for thermal protection of firefighters' gloves with phase change materials

Susan S. Xu, Jonisha Pollard & Weihuan Zhao

To cite this article: Susan S. Xu, Jonisha Pollard & Weihuan Zhao (2025) Three-dimensional heat and moisture transfer analysis for thermal protection of firefighters' gloves with phase change materials, International Journal of Occupational Safety and Ergonomics, 31:1, 214-230, DOI: 10.1080/10803548.2024.2424043

To link to this article: https://doi.org/10.1080/10803548.2024.2424043

INTERNATIONAL JOURNAL OF OCCUPATIONAL SAFETY AND ERGONOMICS (JOSE)
2025, VOL. 31, NO. 1, 214–230
https://doi.org/10.1080/10803548.2024.2424043

Taylor & Francis
Taylor & Francis Group

Three-dimensional heat and moisture transfer analysis for thermal protection of firefighters' gloves with phase change materials

Susan S. Xu [a], Jonisha Pollard [a] and Weihuan Zhao [b]

[a]National Personal Protective Technology Laboratory, National Institute for Occupational Safety and Health, USA; [b]Gregg Wadley College of Science & Health Professions, Northeastern State University, USA

ABSTRACT

Transient three-dimensional (3D) heat and moisture transfer simulations were conducted to analyze the thermal performances of the entire phase change material (PCM) integrated into firefighters' gloves. PCM was broken down into several segments to cover the back and palm of the hand but to avoid finger joints to keep hand functions. Parametric studies were performed to explore the effects of PCM melting temperatures, PCM locations in the glove and PCM layer thicknesses on the overall thermal performance improvement of firefighters' gloves. The study found that PCM segments could extend the time for hand skin surfaces (areas covered or not covered by PCM) to reach second-degree burn injury (60 °C) by 1.5–2 times compared to conventional firefighters' gloves without PCM. Moreover, PCM segments could help mitigate the temperature increase on hand skin and glove surface after fire exposure.

KEYWORDS

structural firefighters' gloves; thermal protective performance; 3D heat transfer modeling; 3D heat transfer simulations; phase change material

1. Introduction

Firefighters are exposed to a wide range of thermal conditions, including flashover conditions in which the air temperature may reach 300–1000 °C with a thermal radiation flux of 15–120 kW/m^2, and hazardous conditions that may have air temperatures up to 250 °C with a thermal radiation flux of 1–10 kW/m^2 [1]. In addition, the glove is one of the thinnest/weakest components of firefighter turnout gear compared to jackets, suits and pants due to the need for hand dexterity and hand grip strength to complete tasks. Typical firefighters' gloves have four layers: the inner thermal lining, a flame-retardant thermal barrier, a moisture barrier and a fireproof leather outer shell [2]. The current structural firefighters' gloves must satisfy the minimum requirement of a thermal protective performance rating of 35, equating to 17.5 s until second-degree burns occur in a flashover situation, to comply with the National Fire Protection Association (NFPA) 1971 Standard on protective ensembles for structural fire fighting and proximity fire fighting [3]. However, exposure to a high-temperature environment could be much longer than a few seconds when firefighters are conducting rescue tasks at a fire scene. In 2021, around 32% of firefighter injuries in the USA were from the fireground (i.e., 19,200 injuries) [4]. Thermal burn and thermal stress were among the major fireground injuries, which accounted for approximately 10% of total fireground injuries [4]. Hence, to maintain protection for much longer exposures to extreme heat without causing burn injuries, it is critical to enhance the thermal protection performance of these gloves.

Firefighters need gloves that meet heat resistance criteria while still fitting correctly and enabling dexterity. The current advanced textile technology, such as special leather materials, elastomeric pillars on fire-resistant fabrics, nanocomposite technology, etc. [5–8], can improve the material insulation performance. However, the improvement is purely based on the delay of conductive heat transfer. The use of phase change material (PCM) can help mitigate the limitation from conduction and significantly enhance the insulation performance of gloves. PCM needs to absorb a large amount of latent heat of fusion to change the phase (e.g., melt), while it maintains at a constant temperature. Applying this phenomenon of PCM to an extreme heat environment, it can absorb the heat for melting and, therefore, significantly reduce the thermal transport rate to hand skin for efficient temperature control and thermal protection. The PCM can utilize its large latent heat to achieve thermo-regulation. Additionally, adding a thin PCM layer to firefighters' gloves allows for smooth hand movements without adding bulk.

Some researchers have investigated microencapsulated PCMs or PCM packs for thermo-regulation in everyday clothing or protective garments for thermal control [9,10]. Microencapsulated PCM is PCM housed in capsules ranging in size from nanoscale to microscale, while a PCM pack is PCM in a macroscale package. Pause [11] explored a new approach to incorporate PCM into non-woven protective garments. The PCM was directly incorporated into a polymer film, and then laminated to a non-woven fabric system [11]. It was found that using PCM can delay the skin temperature increase, reducing the moisture build-up in the microclimate, which improves the thermo-physiological wearing comfort of non-woven protective garments [11]. Lu et al. [12] developed a novel personal cooling system by incorporating PCM packs and ventilation fans in clothes. These studies found that incorporating PCMs with melting points in the range of 15–35 °C in garments could help improve human thermal comfort when wearing protective garments and in daily life [9–12].

Unlike everyday clothing and protective garments, firefighters' personal protective equipment (PPE) is exposed to extremely high temperature conditions. Hence, it is critical to enhance the thermal insulation performance of PPE to

CONTACT Susan S. Xu mxu9@cdc.gov

protect firefighters. Some researchers have experimentally investigated thermal protection by integrating microencapsulated PCMs or PCM layers in firefighters' protective clothing (FFPC) for thermal protection under harsh conditions. It was found that using microencapsulated PCMs could reduce the temperature rise behind the innermost layer by around 5–8.5 °C and increase the thermal protection of FFPC samples by approximately 40% under radiant heat exposure at 5–40 kW/m^2 [13,14]. The PCM with a melting point range of 47–53 °C had the highest heat protection index under such heat flux exposure [15]. Moreover, the effect of PCM was more pronounced when the PCM (melting point of 50 °C) coated layer was placed in the inner layer of FFPC [13]. However, it was found that the PCM did not perform effectively once the environment reached flashover conditions (air temperature of 300–1000 °C) [14,16]. Further parametric studies are required for PCM to improve its performance under extreme heat conditions.

For the aforementioned reasons, numerical simulation work becomes critical to provide time and cost-effective systematic investigations. Several numerical studies related to using PCM for thermal protection in the FFPC ensemble have been reported. For example, Hu et al. [17], Fonseca et al. [18,19] and Zhang et al. [20] have performed one-dimensional (1D) simulations for parametric studies on the effects of PCM mass, position, melting temperature and latent heat on the firefighter clothing thermal performance under various heat intensity conditions (from 5 to 84 kW/m^2; low heat intensity to flashover condition). Moreover, Fonseca et al. [19] have also modeled the thermal transport performance of firefighter clothing after fire exposure. The heat stored in PCM can extend the time that a firefighter is protected in the fire scene before a second-degree burn occurs. However, the accumulated energy in PCM will be eventually released toward the environment and the firefighter's body after coming out of the fire scene, making the post-fire exposure behavior of PCMs critical. Few researchers have conducted preliminary studies on PCMs for their post-fire exposure behaviors [19].

In an earlier study, the authors conducted 1D numerical simulations to investigate the improvement in thermal protective performance of firefighters' gloves when incorporated with a thin PCM layer [21]. This study found that the optimum melting point of PCM was in the range of 80–140 °C for the hand's thermal protection; the location of the PCM layer should be close to the inner glove's surface for high-heat situations; and the addition of a PCM layer of 0.5–1.0 mm could increase the time for the skin to reach second-degree burn temperature by two to four times when compared to conventional firefighters' gloves without PCM [21].

To better protect firefighters from burn injuries and thermal stress at a fire scene, the authors propose incorporating PCM into the glove to break the ceiling of the thermal protective performance of current commercial firefighters' gloves. Unlike firefighting clothing, a glove is small in volume and asymmetric in geometry, so the actual thermal performance in a three-dimensional (3D) glove would be different from the 1D simulation results. Currently, there are no studies on the entire glove system to explore how PCM can be incorporated in an actual glove. 3D models are not available that accurately simulate the thermal performance of the entire glove and hand system. Therefore, this work is the first 3D numerical simulation to explore the effects of different variables (i.e., PCM melting point, position and thickness) on the thermal insulation performance of the entire firefighters' gloves; and the heat and moisture (including sweat and spray water) transport phenomena in the whole glove on the hand under flashover and hazardous conditions. The numerical modeling and simulations presented here will guide future experimental design and testing.

2. Mathematical modeling and numerical solutions

2.1. Model design – hand model and glove composition

The 3D heat and moisture transfer simulations were conducted using COMSOL Multiphysics (Version 6.1). The 3D model geometry, as shown in Figure 1, involved a human skin portion and a glove structure. Human skin includes the subcutis, dermis and epidermis, and a typical structural firefighter glove comprises a base layer (inner thermal lining), thermal barrier, moisture barrier and outer shell. The PCM can be capsulated and integrated between these layers in the glove structure. In this study, PCM was placed between the base layer and thermal barrier (above base layer [ABL]) and between the moisture barrier and outer shell (beneath outer shell [BOS]) to explore the effect of PCM location on glove thermal performance. Considering hand dexterity, one piece of PCM to cover the entire glove would not be appropriate. Hence, the PCM was broken into several segments to cover the back and palm of the hand while avoiding the finger joints to maintain hand function, as shown in Figure 1(c). Commercial bio-based PCMs (fatty acids) were used in the simulations due to their non-toxic nature [22]. Three different melting points of PCMs were studied: 70, 100 and 150 °C. The melting temperature selection was based on the optimum melting temperature range identified from the authors' previous 1D simulation work [21].

2.2. Heat transfer simulation

Heat transfer simulation explored the thermal protection improvement of firefighters' gloves by applying PCM and the amount of time it took for the hand skin surface to reach skin second-degree burn injury ($\sim$60 °C [1]) when exposed in the fire scene. The model involved bioheat transfer physics. The 3D heat diffusion (energy) equation with blood circulation effect, as expressed in Equation (1), was applied to simulate the thermal transport in glove structure as well as hand skin [21,23,24]:

$$\rho C_p \frac{\partial T}{\partial t} = k\nabla^2 T + \dot{Q}_{bio} \quad (1)$$

where ρ = density; C_p = specific heat; T = temperature; t = time; k = thermal conductivity; $\dot{Q}_{bio}$ = bioheat source term indicating heat transfer by blood circulation (which was only used in the dermis and subcutaneous layers of the skin, set at zero in the epidermis layer and glove structure). The bioheat source term can be expressed as follows [21,23,24]:

$$\dot{Q}_{bio} = \rho_b C_{p,b} \omega_b (T_b - T) + \dot{Q}_{met} \quad (2)$$

where ρ_b = density of blood; $C_{p,b}$ = specific heat of blood; ω_b = rate of blood perfusion in skin; T_b = blood temperature; $\dot{Q}_{met}$ = metabolic heat source [21,23,24].

For PCM, the equivalent heat capacity method was adopted for the phase change simulations in COMSOL Multiphysics. The latent heat of fusion of PCM was integrated into the specific heat, as expressed in Equation (3), for the phase changing

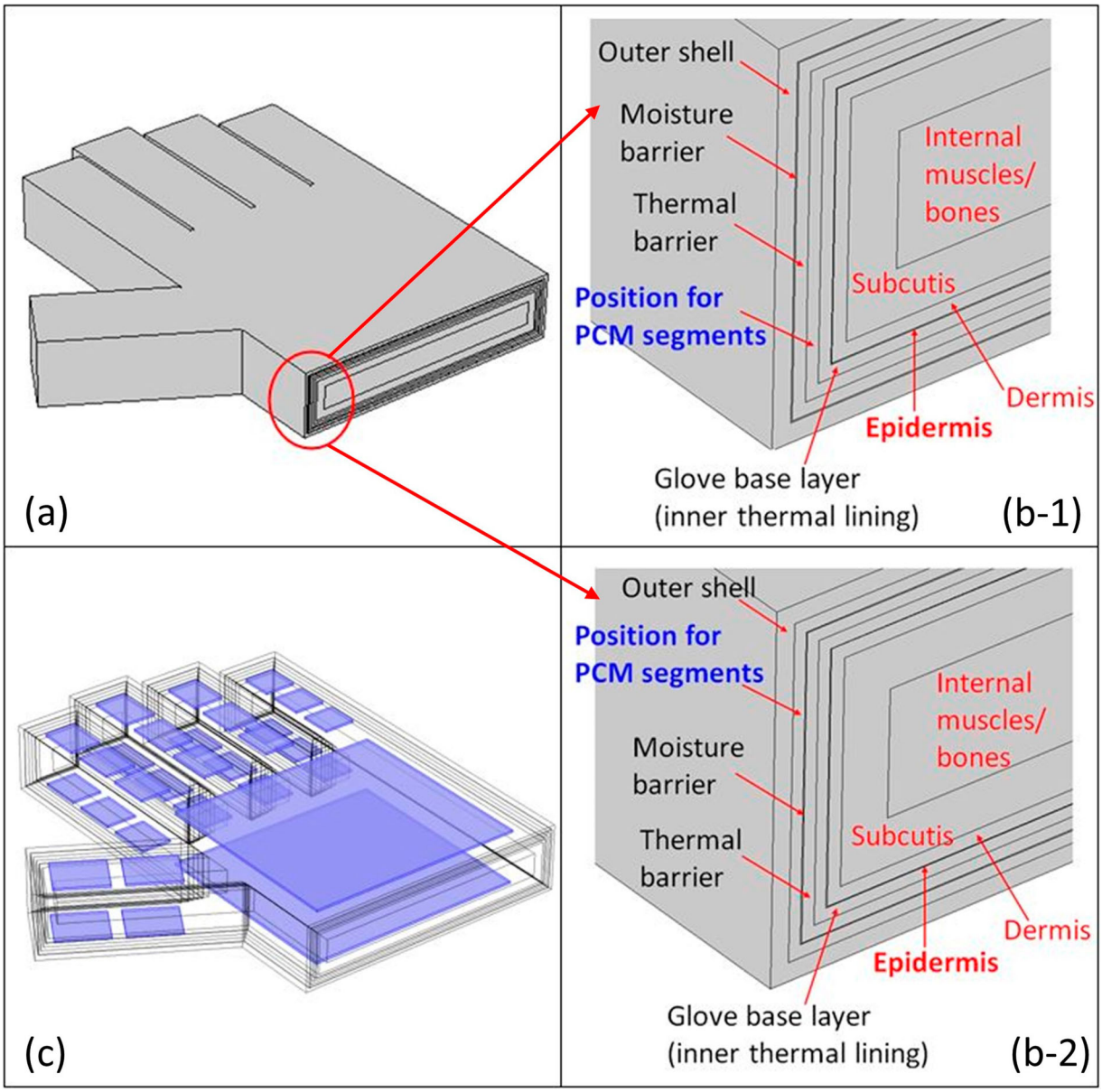

Figure 1. Geometry of the 3D glove–hand model: (a) overall view of the 3D glove–hand model; (b) each glove and skin layer in the model (b-1: PCM located ABL in the glove; b-2: PCM located BOS in the glove); (c) positions of PCM segments in the glove. Note: Air gaps existed between each glove layer as well as between the hand and the glove in the simulation model. (c) Blue parts indicate PCM segments. ABL = above base layer; BOS = beneath outer shell; 3D = three-dimensional; PCM = phase change material.

process [25]:

$$C_p = \frac{1}{\rho}[\rho_s C_{p,s} + (\rho_l C_{p,l} - \rho_s C_{p,s})\mathrm{LF}(T)] + \mathrm{LH}\frac{\partial G}{\partial T} \quad (3)$$

where $C_{p,s}$ and $C_{p,l}$ = specific heat of solid-state and liquid-state PCM, respectively; ρ_s and ρ_l = density of solid-state and liquid-state PCM, respectively; LF(T) = liquid fraction (ranging from 0 to 1) used to determine the change between solid (0) and liquid (1) phases of PCM; LH = latent heat of fusion of PCM; $\partial G/\partial T$ = Gaussian function used to account for the latent heat during phase change. The natural convection in molten PCM was negligible in this study [25].

The parameters and thermal properties of human skin layers, glove materials and PCM are presented in Table 1. The glove layers were modeled as porous materials, whereas human hand skin and PCM were modeled as non-porous materials. Three different melting points (i.e., 70, 100 and 150 °C) of PCMs were simulated in the 3D model to explore the effect of melting points on the thermal performance of PCM-integrated firefighters' gloves. The latent heat of fusion of PCM was assumed to be 200 kJ/kg based on the average latent heat of commercial bio-based PCMs [22].

2.2.1. Initial conditions

The initial temperature of the glove layers was assumed to be room temperature (25 °C). The initial temperature distributions in skin layers are presented in Table 2. The subcutis is close to the body, so it was assumed to be equal to internal body temperature (37 °C) [21,24]. The epidermis faces the outside environment, lowering the skin temperature to 34 °C [21,24]. There is always a temperature gradient from the body core to the skin surface even when gloves and clothes are worn. Hence, the skin surface temperature was slightly lower than that of the body core temperature [24]. The temperature distribution in hand skin is almost linear [21,24].

Table 1. Parameters and thermal properties of human skin and glove layers [22,28,29,31,32,37,38].

Layer	Thickness (mm)	Density (kg/m^3)	Heat capacity (J/kg·K)	Thermal conductivity (W/m·K)	Porosity (unitless)
Subcutis	3.885	1109	2344	0.293	–
Dermis	1.125	1109	3773	0.582	–
Epidermis	0.075	1109	3968	0.628	–
Base layer (insulated cotton lining)	1	134	1865	0.05	0.885
Thermal barrier (fire-retardant cotton)	1	520	1300	0.1	0.885
Moisture barrier (PTFE)	0.1	2285	1030	0.25	0.814
Outer shell (Kevlar fiber)	1.5	567	1300	0.8	0.666
PCM layer (bio-based fatty acids)	0.5-1	1000	2000	0.2	–

Note: PCM = phase change material; PTFE = polytetrafluoroethylene.

Table 2. Initial conditions of hand skin and glove layers for heat transfer simulation [21,24].

Parameter	Subcutis	Dermis	Epidermis	All glove layers
Temperature (°C)	37	35	34	25

2.2.2. Boundary conditions

The outer surface of the gloves' outer shell was set at a heat flux of 83 or 8.3 kW/m^2 to mimic flashover or hazardous conditions, respectively [1]. The temperature at the interface between the hand subcutis and internal muscles/bones was set at a constant 37 °C (the same as the internal body temperature) [21,24]. Moreover, there are air gaps between each glove layer and between the hand skin and glove. These air gaps were assumed to have 0.1-mm thickness for perfectly fitting gloves based on the surface roughness of textile fabrics [26,27].

2.3. Heat and moisture transfer simulation

The Heat Transfer in Porous Media module and the Transport of Diluted Species in Porous Media module were coupled in COMSOL Multiphysics to simulate the heat and moisture transport phenomena in firefighters' gloves. Hand sweating and external water spray from a hose would cause moisture to transfer into the glove. Therefore, this study explores the effect of moisture on the thermal performance of PCM-integrated firefighters' gloves in the cooling period after exposure to the fire scene.

The glove was first heated/exposed under flashover conditions for 4 s and then cooled down until 60 s after the exposure (mimicking when a firefighter gets out of the fire scene) [28]. Two cooling processes were studied, i.e., air-cooled and water-cooled processes. The air-cooled process is for the situation when the firefighter does not use the water hose. Therefore, the glove was just cooled in ambient air. Thus, only hand sweating was considered in the simulation. The water-cooled process is for the situation where a firefighter uses a water hose. Both hand sweating and external water spray from the hose were considered in the simulation.

The governing equation for 3D moisture transfer is expressed as Equation (4) [28]:

$$\epsilon_p \frac{\partial c}{\partial t} = D_{eff} \nabla^2 c \tag{4}$$

where ϵ_p = porosity of glove fabric (refer to Table 1); c = moisture (water vapor) concentration (mol/m^3); D_{eff} = effective diffusion coefficient in porous medium, which is calculated by [29]:

$$D_{eff} = \frac{\epsilon_p}{\tau} D(T) \tag{5}$$

where τ = fabric tortuosity ($\tau = {\epsilon_p}^{-1/3}$); $D(T)$ = diffusion coefficient of water vapor (moisture) in air, which is a function of temperature as follows [30]:

$$D(T) = 1.87 \times 10^{-10} \frac{T^{2.072}}{P_{atm}} \tag{6}$$

where P_{atm} = atmosphere pressure (atm).

The heat diffusion equation is modified into Equation (7), adding the term of enthalpy of vaporization due to moisture mass transfer in the glove structure (Q_{vap}):

$$\rho C_p \frac{\partial T}{\partial t} = k \nabla^2 T + Q_{bio} + Q_{vap} \tag{7}$$

The moisture bonded with textile fibers or in pores would evaporate and condense during the temperature change, leading to the latent heat of vaporization accompanying moisture mass transfer. Hence, Q_{vap} was defined as follows [30]:

$$Q_{vap} = -D_{eff} \nabla^2 c \cdot \Delta H_{vap} \tag{8}$$

where ΔH_{vap} = latent heat of vaporization of water.

Regarding the initial conditions, the initial temperature distributions in the glove and hand skin are the same as in the heat transfer simulation (refer to Table 2). The initial moisture content in the glove structure was assumed to be 0.816 mol/m^3 based on the relative humidity of 60% [28,30].

Regarding the boundary conditions, for heat transfer the flashover condition with a heat flux of 83 kW/m^2 was applied at the outer surface of the glove's outer shell during the first 4-s heating process. Natural convection and radiation cooling were then applied to the outer shell during the cooling process afterward.

The component of natural convection heat flux (Q''_{conv}) was calculated by [31]:

$$Q''_{conv} = h_{conv}(T_s - T_\infty) \tag{9}$$

where T_s = glove outer surface temperature; T_∞ = environment temperature out of fire scene (25°C) [28]; h_{conv} = convective heat transfer coefficient, which was evaluated based on the Nusselt number (Nu) correlation on a vertical plate surface [31]:

$$\mathrm{Nu} = \left\{ 0.825 + \frac{0.387 \mathrm{Ra}^{\frac{1}{6}}}{\left[1 + (0.492/\mathrm{Pr})^{\frac{9}{16}}\right]^{\frac{8}{27}}} \right\}^2 \tag{10}$$

where Ra = Rayleigh number ($\mathrm{Ra} = \frac{g\beta(T_s - T_\infty)L^3}{\nu\alpha}$, here g); Pr = Prandtl number ($\mathrm{Pr} = \nu/\alpha$). Both air-cooled and water-cooled processes were considered for natural convection cooling.

Table 3. Parameters to calculate natural convection and radiation heat transfer coefficients [28,32].

Parameter	Air (at 750 K)	Water (at 300 K)
Kinematic viscosity, ν (m^2/s)	7.637×10^{-5}	8.58×10^{-7}
Thermal diffusivity, α (m^2/s)	1.09×10^{-4}	1.47×10^{-7}
Thermal expansion coefficient, β (K^{-1})	1.33×10^{-3}	2.761×10^{-4}
Prandtl number, Pr	0.702	5.83
Length of glove, L (mm)	200	
Emissivity of glove outer shell material, ε	0.725	
Stefan-Boltzmann constant, σ ($W/m^2 \cdot K^4$)	5.67×10^{-8}	

Note: The Pr number is a dimensionless number that compares the transport between momentum and thermal diffusivities, i.e., $\Pr = \nu / \alpha$.

The component of radiation heat flux (Q''_{rad}) was expressed as follows [32]:

$$Q''_{rad} = h_{rad}(T_s - T_\infty) \tag{11}$$

where h_{rad} = radiation heat transfer coefficient, i.e., $h_{rad} = \varepsilon\sigma(T_s^2 + T_\infty^2)(T_s + T_\infty)$ [31].

Table 3 presents the properties of air and water and other parameters to calculate the natural convection and radiation cooling boundary conditions using Equations (9)–(11).

For moisture transfer, the water vapor would transport through glove fabric layers (the porous materials) but would not be able to pass through the PCM layer (non-porous material). At the hand skin surface (surface of epidermis), the human hand sweating flux was defined as 0.014 $mol/m^2 \cdot s$, calculated based on the maximum human sweating rate of 15 $g/min\ m^2$ [33–35]. On the outer surface of the glove's outer shell, the moisture mass flux ($\dot{m}$) was defined as follows [28]:

$$\text{In the heating process, } \dot{m} = h_{air}(c_{amb,air} - c) = h_{air}(0 - c) \tag{12}$$

$$\text{In the air - cooled process, } \dot{m} = h_{air}(c_{amb,air} - c) = h_{air}(0.816 - c) \tag{13}$$

where h_{air} = convective mass transfer coefficient in ambient air, with the value of 0.021 m/s [28]. In the heating process, due to the extremely high heat flux to mimic flashover conditions, the moisture content in ambient air ($c_{amb,air}$) was assumed to be negligible (zero). In the air-cooled process, the moisture content in ambient air ($c_{amb,air}$) was assumed to be at a relative humidity of 60% (0.816 mol/m^3) [28,30].

For the water-cooled process, the moisture mass flux on the outer surface of the glove was based on external water spray from a hose. This work assumed 10 times the hand sweating rate, leading to 0.14 mol/m^2 s.

2.4. Numerical solution reading points and mesh for modeling

The numerical solutions were calculated through solving the governing equations – heat diffusion equation (Equation (1)) and coupled heat and moisture transfer equations (Equations (4) and (7)) along with the initial and boundary conditions in COMSOL Multiphysics. The built-in time-dependent solver with backward differentiation formula (BDF) of COMSOL Multiphysics was utilized to obtain the temperature and moisture concentration solutions with respect to time. Based on the temperature data, the time for hand skin surface to reach second-degree burn injury (60 °C) could be determined. The flow chart for the numerical solution procedure is shown in Figure 2.

To export the temperature and moisture concentration profiles from COMSOL Multiphysics and explore the temperature control performance of PCM-integrated firefighters' gloves, we created nine probes at different positions in the glove geometry and on the hand skin, as shown in Figure 3. Probes 1–6 were located on the human skin surface to collect the skin temperature and seek the time to reach the second-degree burn injury in this study. Probe 2 was the location of the finger joint, which was not covered by the PCM segment. Probes 1–3 were on the finger, while Probes 4–6 were on the palm. Probe 7 was on the inner surface of the PCM encapsulation, while Probe 8 was on the outer surface of the PCM encapsulation. Probes 7 and 8 provided information on the phase change status of the PCM. These two probes were absent from the glove with no PCM integrated. Probe 9 was located at the outer surface of the glove's outer shell.

Figure 4(a) shows the mesh structure in the glove–hand model. Free tetrahedral elements were used to create the mesh structure for the model. The normal element size in COMSOL Multiphysics was chosen, leading to 310,486 domain elements, 114,470 boundary elements and 8710 edge elements. The meshing size was found sufficient for the heat and moisture transfer simulations based on a mesh independence study for the entire glove–hand model shown in Figure 4(b).

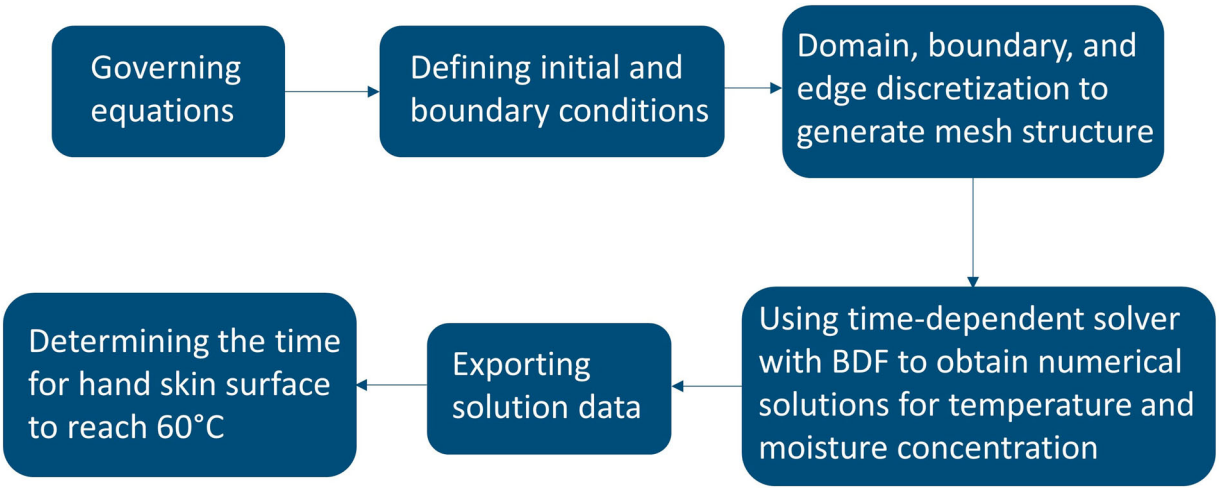

Figure 2. Flow chart for numerical solution procedure. Note: BDF = backward differentiation formula.

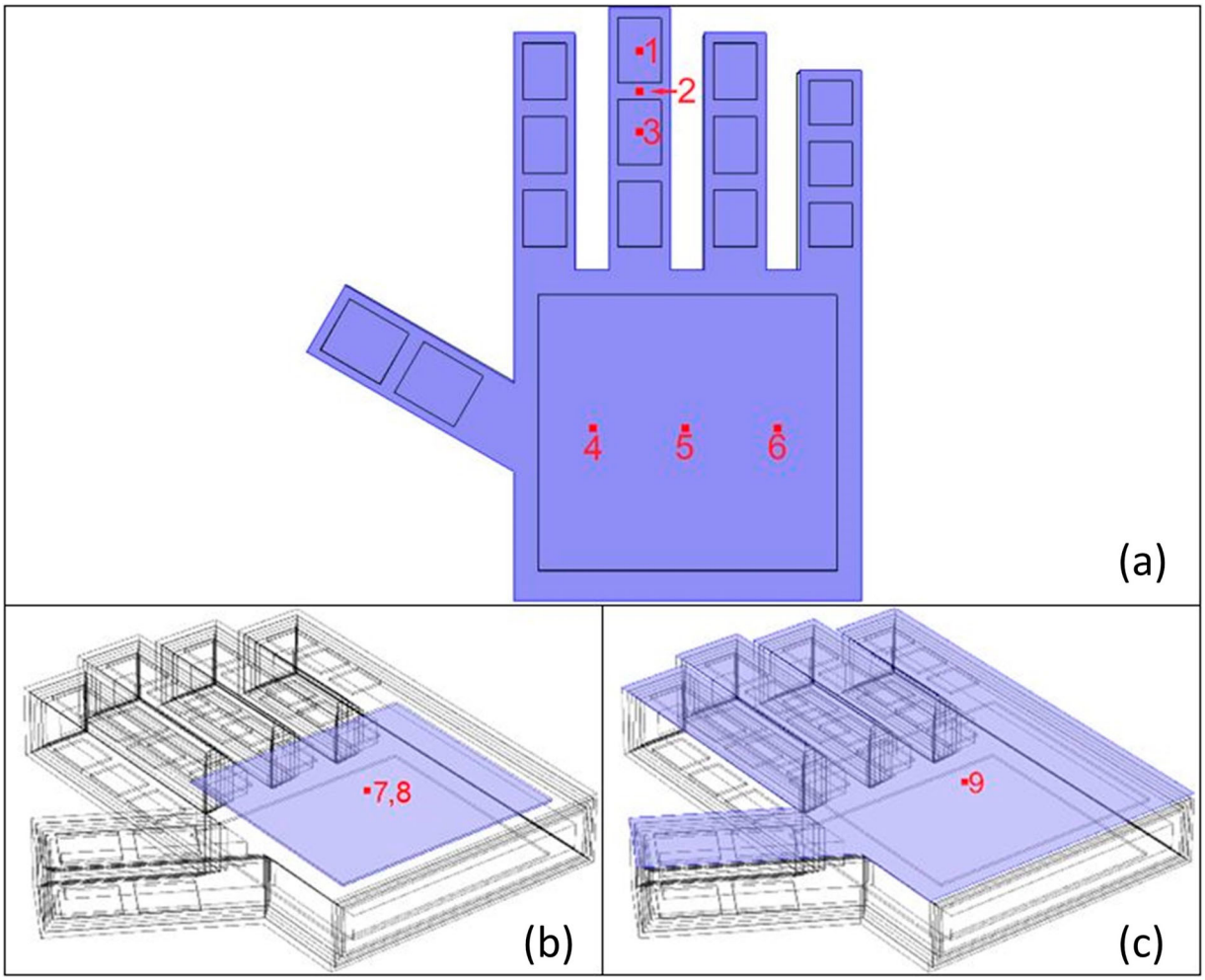

Figure 3. Probe locations in the model to export temperature and moisture concentration profiles after simulation: (a) Probes 1–6 measure hand skin surface temperatures; (b) Probes 7 and 8 measure the data on the inner and outer surfaces of the PCM segment, respectively; (c) Probe 9 measures the temperature on the outer surface of the outer shell of the glove. Note: PCM = phase change material.

Fine element size analysis provided similar simulation results (see temperature profiles in Figure 4(b)), but its computational time was much longer compared to the normal element size.

2.5. Parametric evaluation of PCM in firefighters' gloves

A parametric study was conducted to evaluate how PCM influenced the overall thermal protective performance of firefighters' gloves. The parameters include PCM melting point, PCM location and PCM thickness. This study aimed to identify the optimum PCM property, configuration and geometry to achieve a better thermal protective performance of glove.

3. Results and discussion

3.1. Heat transfer analysis for PCM-integrated firefighters' gloves

Figure 5 shows the phase transition process of PCM segments in firefighters' gloves under exposure at a flashover condition (heat flux at 83 kW/m^2). The PCM segments had a melting temperature of 70 °C, were 1 mm thick and were located ABL. The number zero (0) in Figure 5(a)–(d) represents the solid state of PCM, while the number one (1) represents the liquid state of PCM. Most of the PCM was still in the solid state at the early heating stage, as shown in Figure 5(a). However, as time went on, more and more PCM turned into a liquid state by absorbing a large amount of heat during the heating process. Because the heat flux was applied at the outer surface of the glove, the PCM melted from outside to inside. During the melting process, the PCM could absorb the heat but maintain a relatively constant temperature, which helped to achieve efficient temperature control for hand skin protection. Hence, the glove's outer surface temperature rose rapidly beyond 1000 °C. However, the inside glove layers still maintained below 44 °C (the threshold temperature of pain [1]) after 25 s of heating at 83 kW/m^2, as shown in Figure 5(e) and (f).

The PCM segments had a melting temperature of 70 °C, were 1 mm thick and were located ABL. Temperature profiles on the hand skin surface, PCM segment and glove outer surface are shown in Figure 6. This figure compares the temperatures between conventional firefighters' gloves and PCM-integrated firefighters' glove-protected hands to explore the thermal protection improvement by PCM. The times for hand skin (skin area covered by PCM, locations of Probes 1 and 3–6) to reach second-degree burn injury temperature (~60 °C) could be extended by more than two times compared to conventional firefighters' gloves (no PCM), as shown in Figure 6(a) and (c). Even for the hand surface areas (such as the finger joints) that were not directly covered by PCM segments, the time to reach 60 °C was around 1.5 times longer than that for conventional firefighters' gloves (comparing temperatures at the location of Probe 2). Under flashover conditions, the times for hand skin temperature to reach 60 °C were extended from

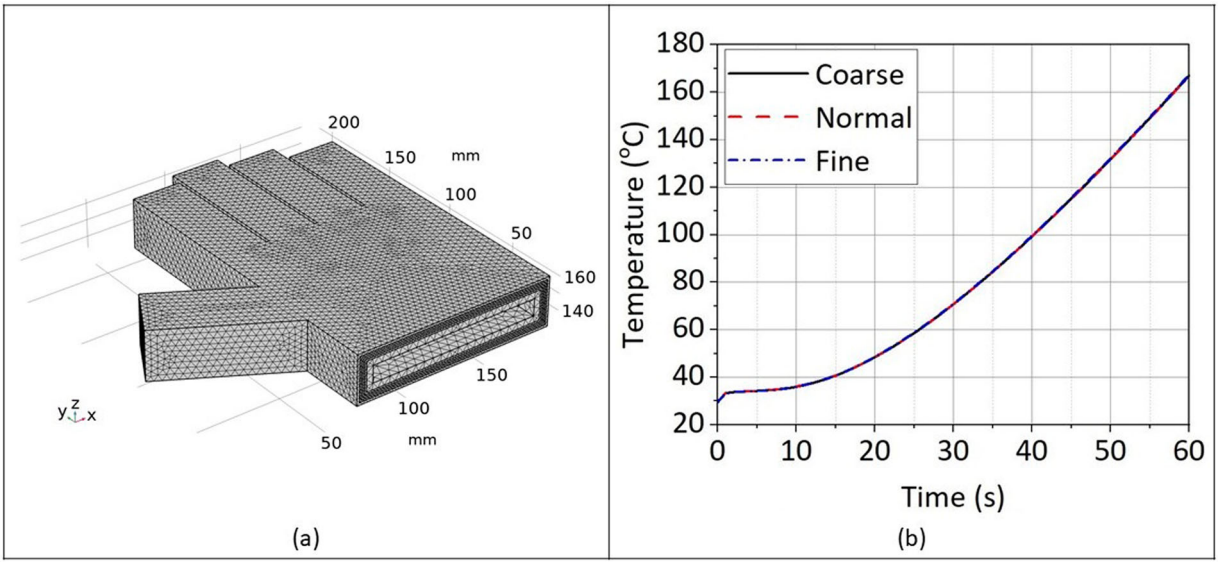

Figure 4. (a) Mesh structure in firefighters' gloves model created by free tetrahedral elements. (b) Mesh independence study on the 3D entire glove–hand model under high-heat condition (temperature data exported from Probe 5 – the hand skin surface temperature at the center of palm). Note: 3D = three-dimensional.

15.5 s (baseline; control) to 26.5–36.5 s (refer to Probes 2 and 5 in Figure 6(a)) when PCM segments were integrated into conventional firefighters' gloves. Under the hazardous condition, the times for hand skin temperature to reach 60 °C could be extended from 63–66 s (baseline; control) to 101–129 s (refer to Probes 2 and 5 in Figure 6(c)) by integrating the PCM segments. The simulation results found that the glove PCM segments could enhance the entire hand's thermal protection by absorbing large amounts of heat during the phase-changing process, even for the areas not covered by PCM. Moreover, the temperature increase rate on the glove's outer shell was slowed down through PCM segments, as shown in Figure 6(b) and (d). Temperatures on the glove's outer surface could be reduced by 50–100 °C after exposure of 30 and 115 s to flashover and hazardous conditions, respectively, when integrating PCM in firefighters' gloves.

Figure 7 shows a parametric study of the effects of PCM melting point, PCM location and PCM thickness on the thermal protective performance enhancement of firefighters' gloves. As with the baseline (control group), the times for the hand skin surface to reach second-degree burn injury under conventional firefighters' gloves (no PCM involved) were 15.5 and 63–66 s under flashover and hazardous conditions, respectively.

3.1.1. PCM melting temperature effect

Three melting temperatures of PCMs were studied: 70, 100 and 150 °C. The melting points of 70 and 100 °C showed better thermal protective performance in gloves than the 150 °C melting point PCM (Figure 7). The 100 °C melting point PCM could also help the hand skin (area covered or not covered by PCM segments) hold the longest time to reach second-degree burn injury. The performance of 70 °C melting point PCM was close to that of 100 °C melting point PCM – sometimes only having a difference of 1–2 s. The time to reach second-degree burn injury could be shortened by up to 7 s when using a 150 °C instead of a 100 °C melting temperature PCM. The effect of PCM melting temperature was more profound under hazardous conditions.

3.1.2. PCM location effect

Under flashover conditions (heat flux of 83 kW/m^2), the skin area covered by PCM (Probe 5) was protected better when PCM was located inside (ABL), compared to that located BOS. The PCM could melt very fast when located close to the outer environment under the high heat flux. It would quickly convert to the liquid state and lose the benefits of the phase change function. Hence, moving the PCM segment toward the inside of the glove (close to the hand) could reduce the high heat flux effect, and therefore extend the melting (phase change) time for better hand protection. It was found that the time to reach second-degree burn injury could be extended by 1–3 s when PCM was located ABL, compared to the BOS location.

Under hazardous conditions (heat flux of 8.3 kW/m^2), the skin area covered by PCM (Probe 5) was protected better when PCM was located BOS, compared to that located close to the hand (ABL). The PCM could melt slower when the outside heat flux was lower, maintaining a longer time at a solid state. Thus, the phase change function was not efficient. A more efficient phase change function could be achieved when the PCM was located close to the outer environment. The time to second-degree burn injury could be extended by 3–10 s by moving the PCM from ABL to BOS in a hazardous condition. These phenomena were consistent with those obtained from previous 1D simulation results [20]. For the area not covered by PCM segments (e.g., location of Probe 2), the time to second-degree burn injury could be extended by 1.5–6 s when PCM segments were located BOS, compared to the ABL location, for both flashover and hazardous conditions.

3.1.3. PCM thickness effect

As shown in Figure 7, the thicker PCM had better thermal protection performance than the control group (firefighters' gloves with no PCM). A PCM segment 0.5 mm thick could help extend the thermal protection time by 5–10 and 17–36 s under flashover and hazardous conditions, respectively; and a PCM segment 1 mm thick could extend the thermal protection time by 10–20 and 35–70 s under flashover and hazardous conditions, respectively.

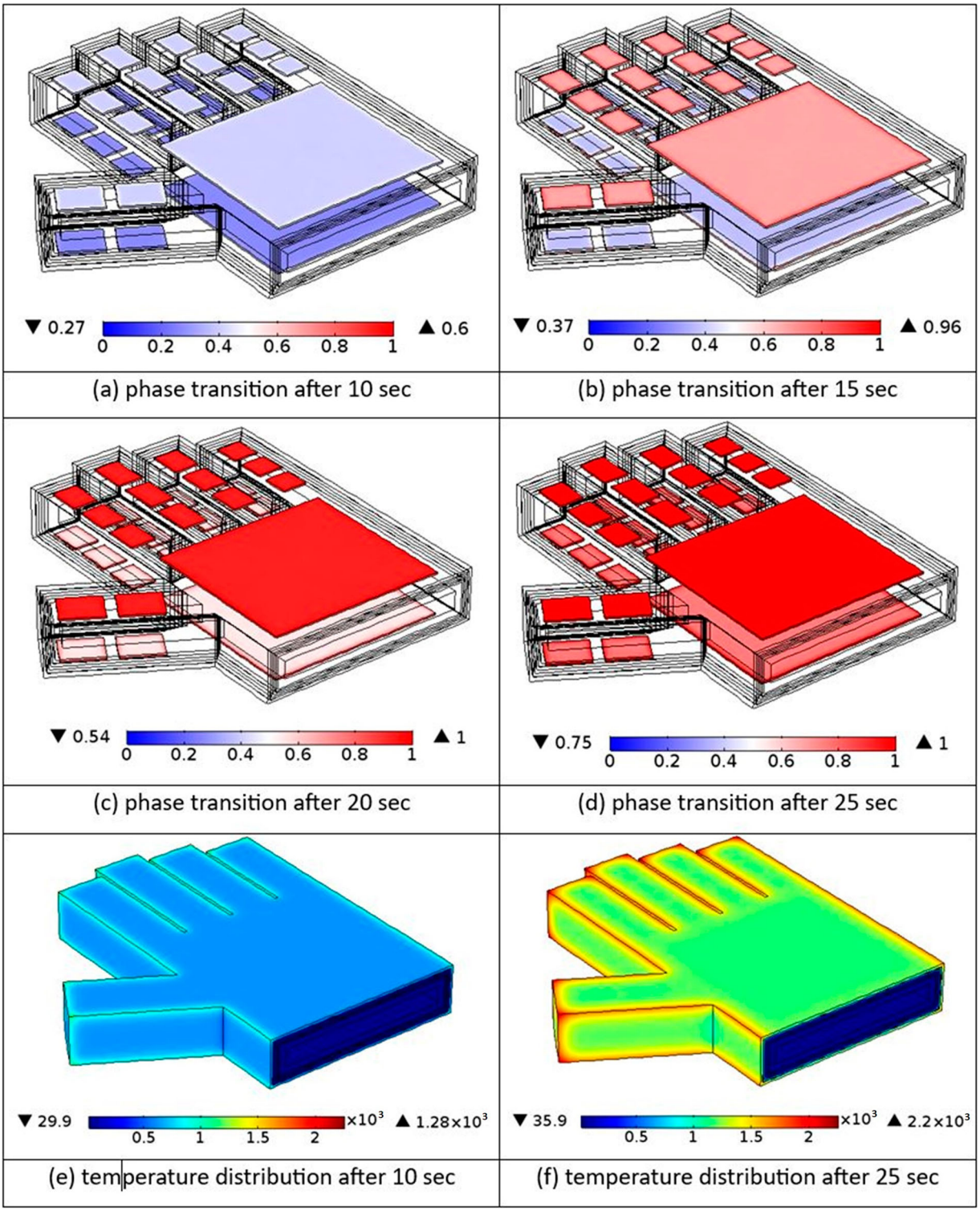

Figure 5. Phase transition process and temperature profiles in PCM-integrated firefighters' gloves under exposure at flashover condition (heating process at a heat flux of 83 kW/m^2): (a)–(d) phase transition process of PCM in glove; (e) and (f) temperature (°C) profiles of PCM-integrated firefighters' gloves after 10 and 25 s of exposure at flashover condition, respectively. Note: (a)–(d) Blue indicates the solid state (0) of PCM, red indicates the liquid state (1) of PCM. PCM = phase change material.

3.2. Heat and moisture transfer analysis during the cooling period

The study of post-fire exposure behaviors of firefighters' gloves is also important. This examines how the stored heat in gloves from a fire scene releases and how the released heat can affect the human hand. The heat released after fire exposure could accompany hand sweating and external spray of water from a hose. Thus, moisture transfer in gloves was considered in this study to explore how moisture could influence hand skin temperature variations. In this study, the PCM segments had a melting temperature of 70 °C, were 1 mm thick and were located between the base layer and thermal barrier (i.e., ABL). Both air-cooled and water-cooled processes were investigated.

Figure 8 shows the temperature profiles on the hand skin surface, embedded PCM and glove outer surface for the air-cooled process after fire exposure. The moisture content in the environment and hand sweating factors were considered in

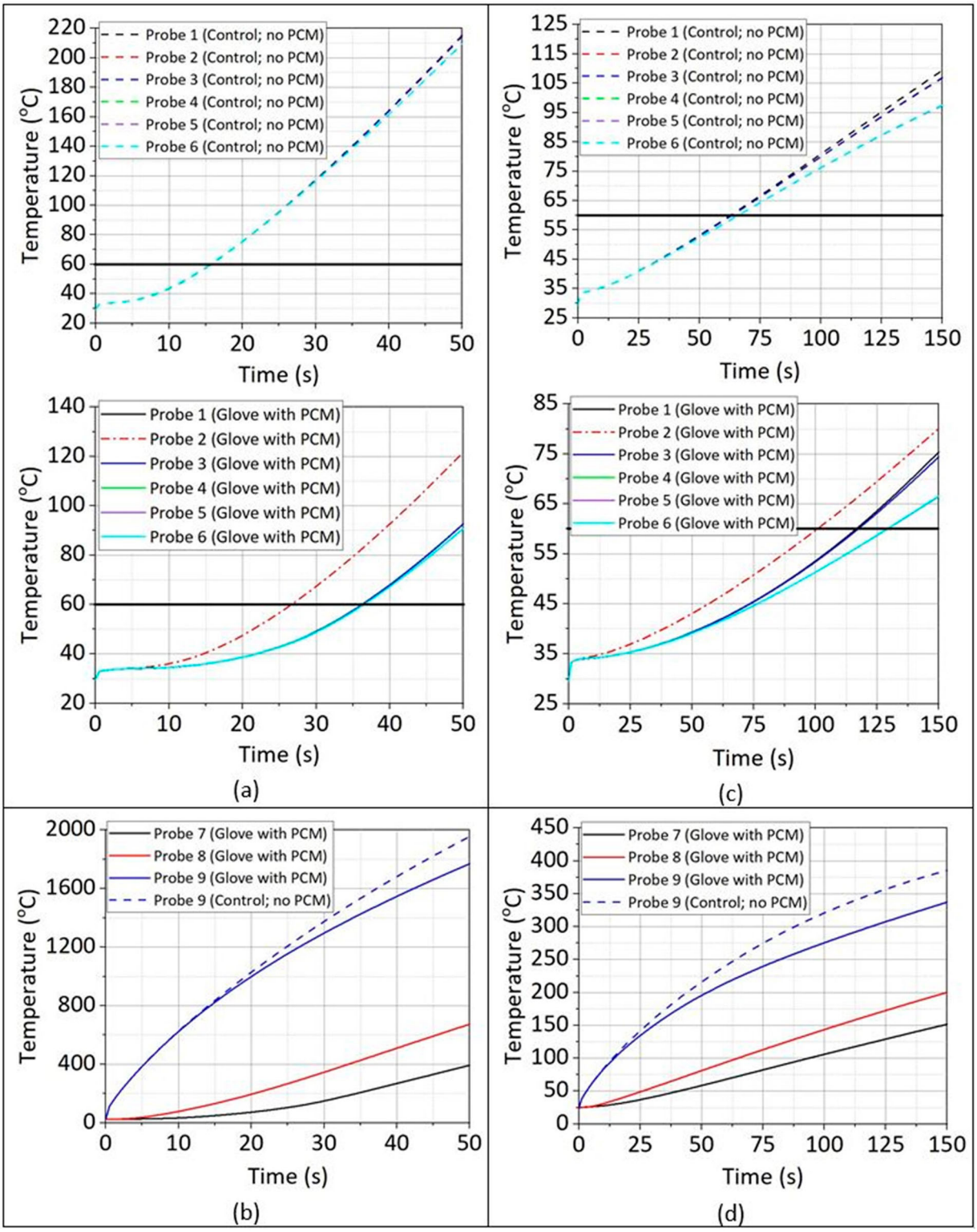

Figure 6. Temperature profiles on the hand skin surface, embedded PCM and glove outer surface: (a) hand skin surface temperatures under flashover condition (heat flux of 83 kW/m^2); (b) embedded PCM and glove outer surface temperatures under flashover condition (heat flux of 83 kW/m^2); (c) hand skin surface temperatures under hazardous condition (heat flux of 8.3 kW/m^2); (d) embedded PCM and glove outer surface temperatures under hazardous condition (heat flux of 8.3 kW/m^2). Note: refer to Figure 3 regarding locations of Probes 1–9. PCM = phase change material.

this simulation. The cooling period occurred after a 4-s exposure under the flashover condition (heat flux of 83 kW/m^2). Figure 8(a) shows that the hand skin temperature did continue to increase even after the 4-s heating process because the stored heat in the glove dissipated toward the surroundings when firefighters came out of the fire scene. Hence, the skin temperature would increase slightly before decreasing due to thermal inertia. The results showed that the hand skin temperature protected by the glove with PCM segments increased more slowly than that protected by the glove without PCM. Even for the area not covered by PCM segments (e.g., Probe 2), the temperature rise was much slower compared to the glove with no PCM. Figure 8(b) displays the inner surface (Probe 7) and outer surface (Probe 8) of the encapsulated PCM segment in the glove. The portion of the PCM closest to the external environment (Probe 8) had undergone phase change. Thus, it maintained the PCM outer surface temperature around 70 °C, effectively maintaining the temperature beneath the PCM

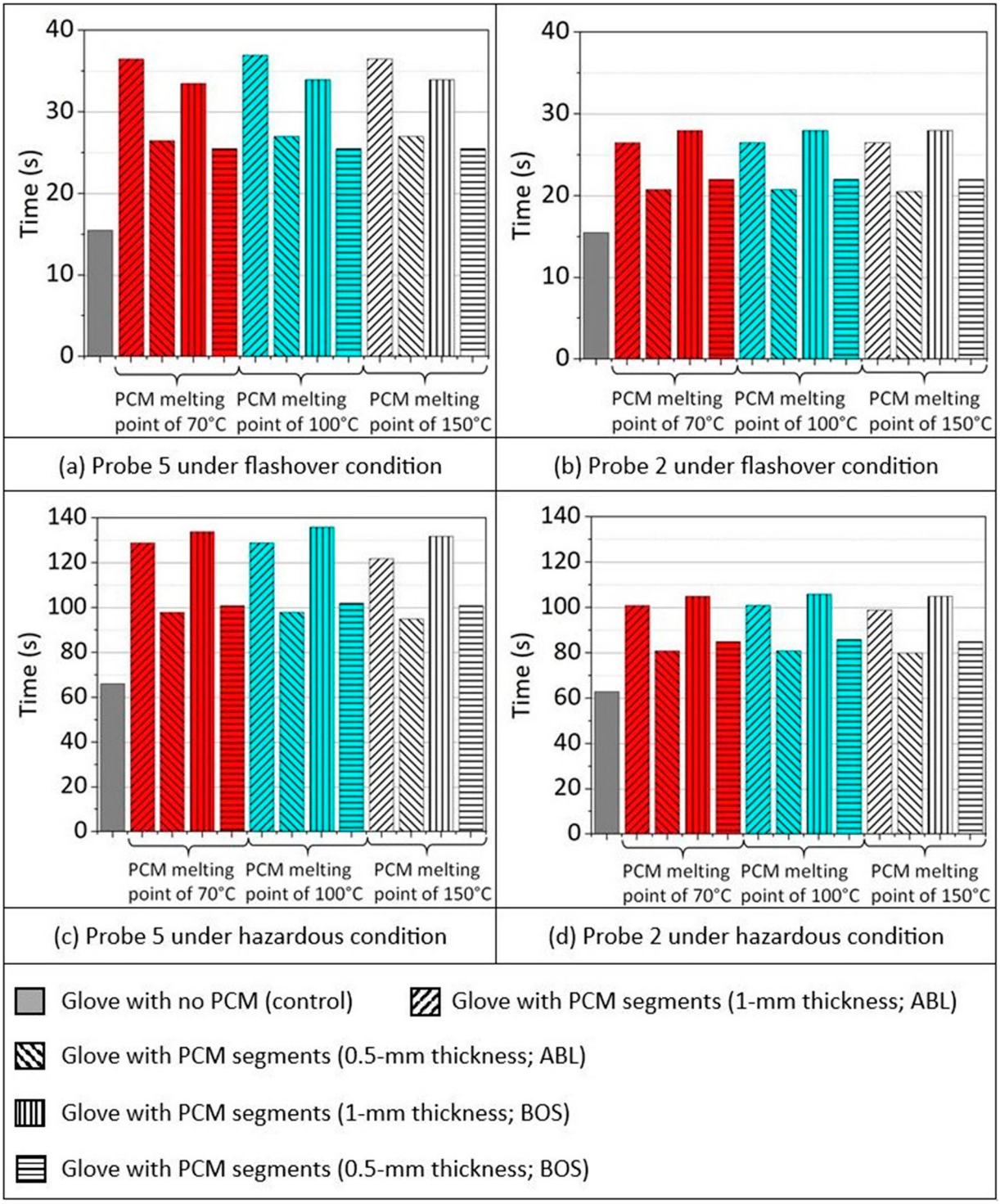

Figure 7. Times for the hand skin surface to reach second-degree burn injury (~ 60 °C): (a) and (b) locations of Probe 5 and Probe 2, respectively, under flashover condition; (c) and (d) locations of Probe 5 and Probe 2, respectively, under hazardous condition. Note: ABL = above base layer; BOS = beneath outer shell; PCM = phase change material.

segments at a lower temperature level compared to the glove with no PCM. Figure 8(c) shows the temperature at the outer surface of the glove's outer shell. The PCM segments could also help reduce the glove's outer surface temperature compared to the glove with no PCM. Therefore, the PCM segments could help improve the temperature control performance of firefighters' gloves even after fire exposure.

Figure 9 shows the results including the external water spray from a hose, which could provide a more efficient cooling process than ambient air. Hence, the temperatures of the hand skin, embedded PCM segment and glove's outer shell surface were much lower than those from air cooling only. The effect of PCM segment protection was insignificant as the temperatures reduced faster for water cooling. Nevertheless, PCM segments could still help mitigate the peak temperature increase after fire exposure (Figure 9(a)).

Figure 10 shows the moisture concentration on the hand skin at the finger joint (Probe 2) during the cooling period. For the air-cooled process (Figure 10(a)), the moisture concentration was from hand sweating and humidity in ambient air (i.e., relative humidity of 60%). Because PCM segments are non-permeable material, the embedded PCM could affect the permeability of the glove. The hand skin with PCM-integrated glove protection showed higher moisture concentration than

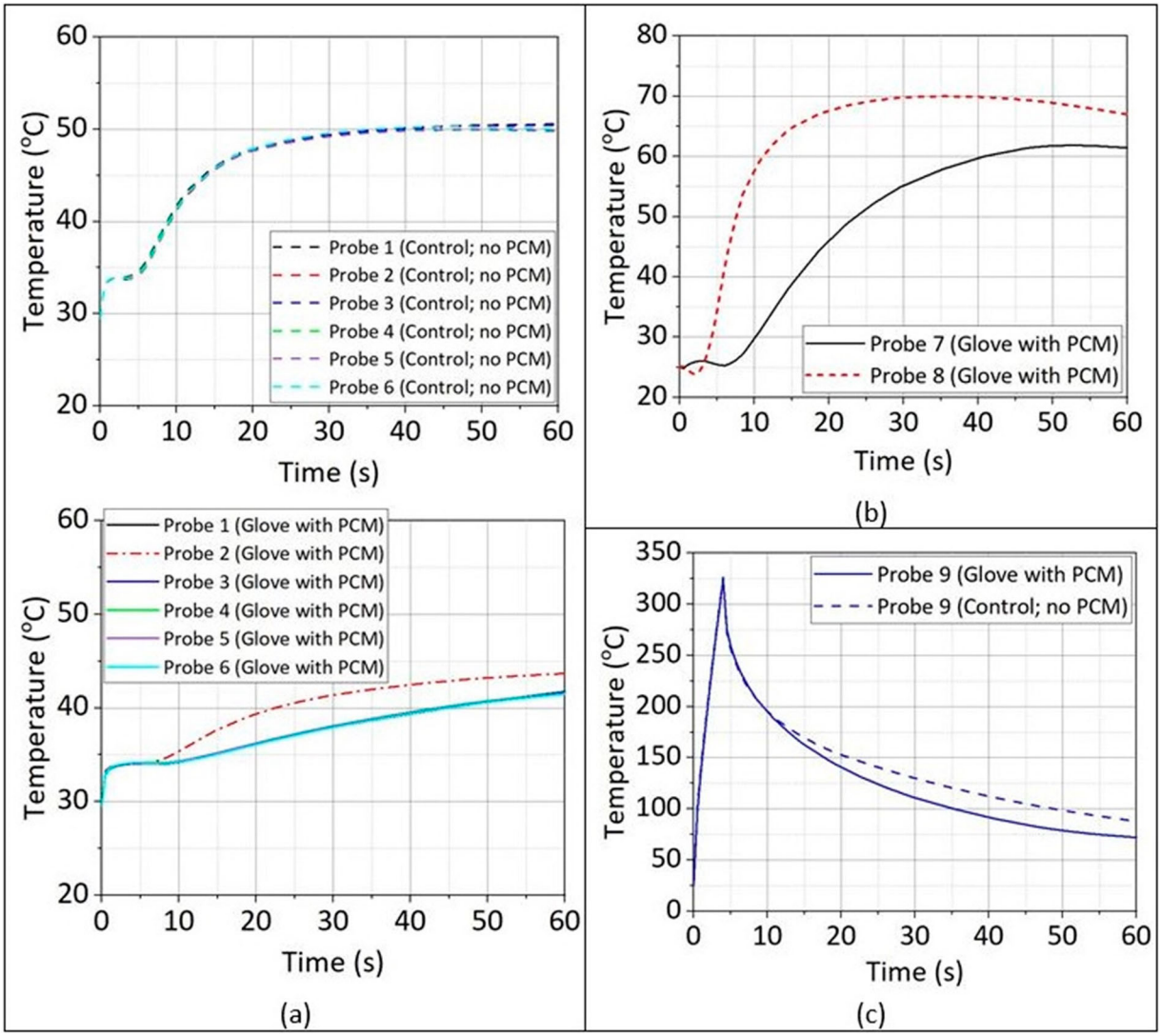

Figure 8. Temperature profiles at (a) hand skin surface, (b) embedded PCM and (c) glove outer surface during the cooling period after fire exposure, considering the effects of hand sweating and moisture content in the environment. The glove was cooled by ambient air only. Note: PCM = phase change material.

conventional firefighters' gloves with no PCM because the PCM segments slowed down the moisture dissipation of hand sweat toward the outside. The increase of moisture concentration on hand skin was not significant, resulting in only a 1–2 mol/m^3 increase. Similar phenomena were observed for the water-cooled process (Figure 10(b)). The major moisture transfer direction was from the outside to the inside because the water spray was from the glove's outer surface. The PCM segments slowed down the moisture transport from the external spray water, resulting in a lower concentration on the hand skin.

More detailed moisture concentration distributions in gloves are shown in Figures 11 and 12 for PCM-integrated and conventional firefighters' gloves, respectively. The PCM segment is a non-porous material, which does not allow water vapor to pass through directly. Hence, moisture could be accumulated on one side of the PCM segment, as shown in Figure 11. However, because PCM segments were used instead of a whole piece of PCM in the glove, moisture from hand sweating could still dissipate outside through the areas not covered by PCM to maintain the permeability of firefighters' gloves. The moisture concentration gradients could be observed around PCM segments in Figure 11(a)–(d), indicating the moisture transport direction in the glove to dissipate the hand sweat.

The primary moisture transfer direction was from the outer surface to the inside of the glove when using external water spray from the hose for cooling (water-cooled process). Hence, the moisture concentration was higher on the glove's outer surface, and lower inside, especially in the palm area, due to the large PCM segment covered, as shown in Figure 11(e). For conventional firefighters' gloves, the moisture concentration distribution was more uniform throughout the entire glove. There was no accumulated moisture in the glove, as shown in Figure 12.

4. Limitations and validation of the simulation model

4.1. Limitations

The 3D simulation model predicts the overall thermal and moisture transport performance in firefighters' gloves. Due to the limitation of establishment for complex geometry, it is challenging to create an exact hand geometry in COMSOL Multiphysics. COMSOL Multiphysics used rectangular configurations to generate the glove-hand model, which involves a 90° angle around fingers and the hand instead of smooth curved surfaces. As a result, it could create some degree of simulation inaccuracy around these angles. Nevertheless, these

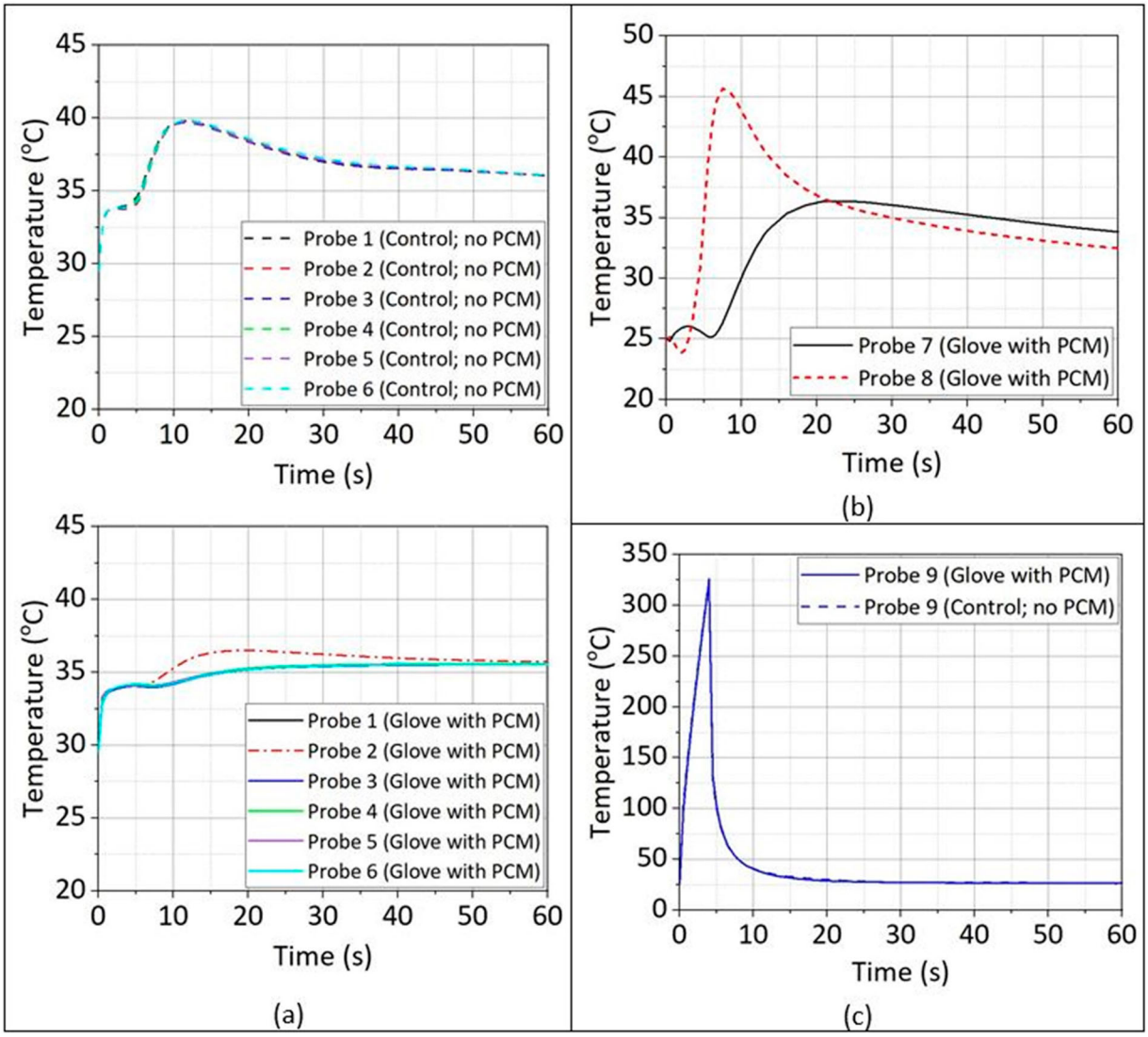

Figure 9. Temperature profiles at (a) hand skin surface, (b) embedded PCM and (c) glove outer surface during the cooling period after fire exposure, considering the effects of hand sweating, the moisture content in the environment and external water spray from a hose. The glove was cooled with water spray. Note: PCM = phase change material.

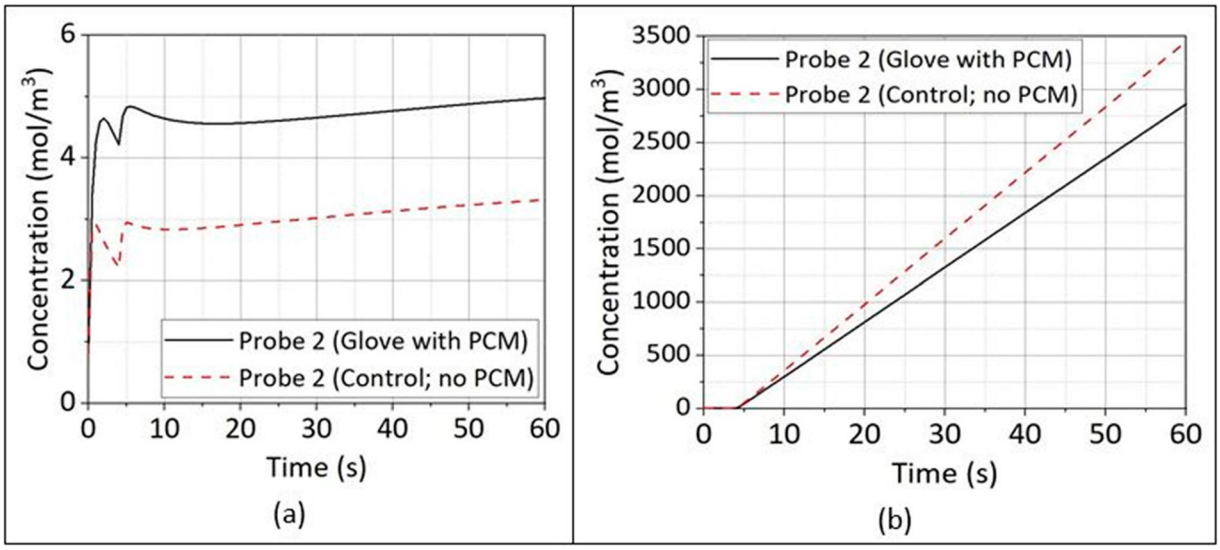

Figure 10. Moisture concentration on the hand skin surface at the finger joint (Probe 2) during the cooling period: (a) glove cooled by ambient air; (b) glove cooled by water spray. Note: PCM = phase change material.

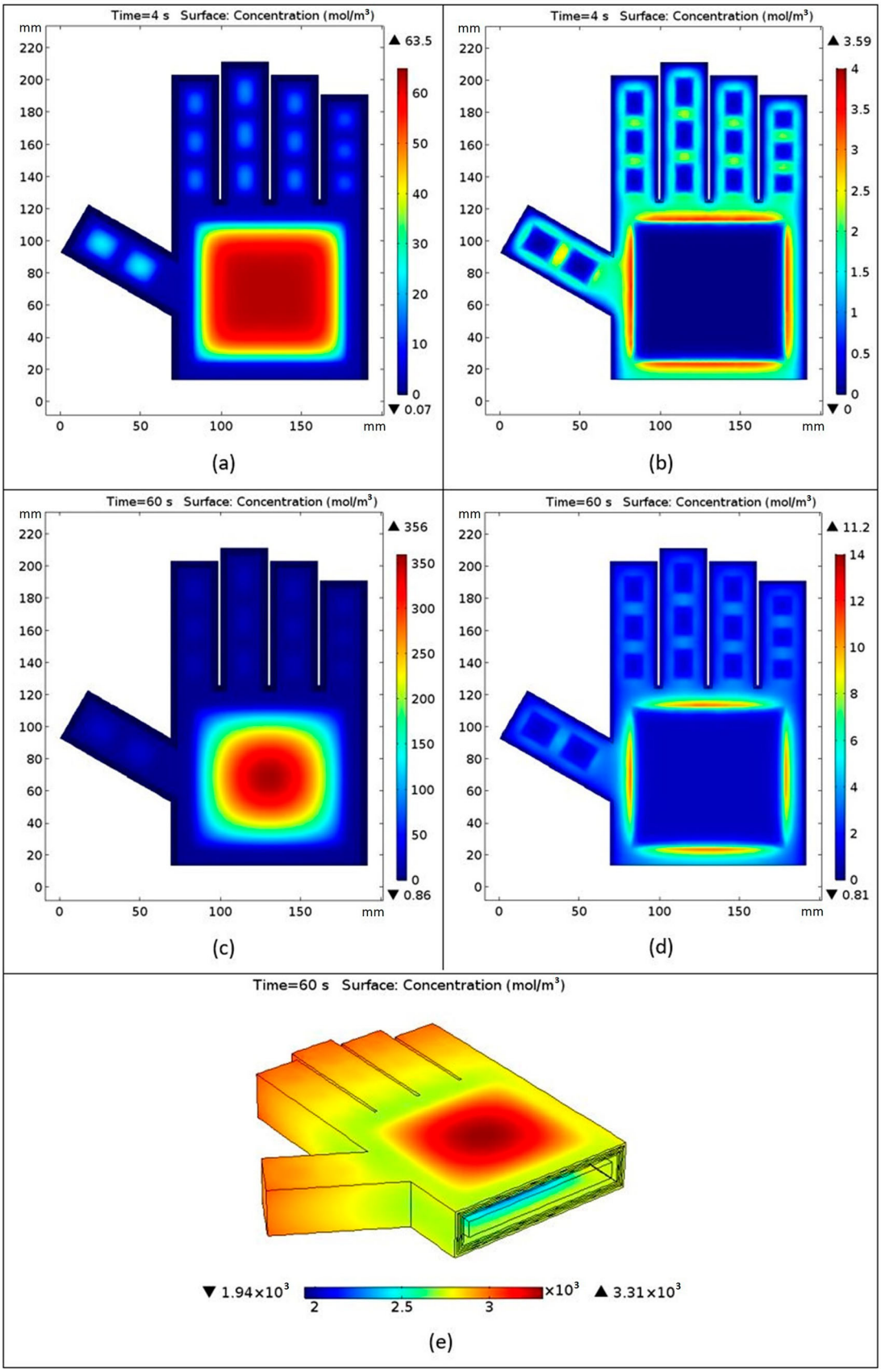

Figure 11. 3D illustration of moisture concentration distribution in PCM-integrated firefighters' gloves: (a) view at the cut plane of the inner surface of PCM segments after 4-s fire exposure; (b) view at the cut plant of the outer surface of PCM segments after 4-s fire exposure; (c) view at the cut plane of the inner surface of PCM segments after 60-s air cooling period; (d) view at the cut plant of the outer surface of PCM segments after 60-s air cooling period; (e) 3D view of the entire glove after 60-s water cooling period. Note: 3D = three-dimensional; PCM = phase change material.

angles do not affect the overall simulation results for the entire hand and glove point of view, resulting in reasonable numerical predictions. Moreover, the hand skin was assumed to be non-porous material in the simulation. The hand sweating rate was applied as the boundary condition at the surface of epidermis. Although the hand skin was considered to be non-porous material in the model, the thermal properties of hand skin used in the simulation were the effective properties considering the

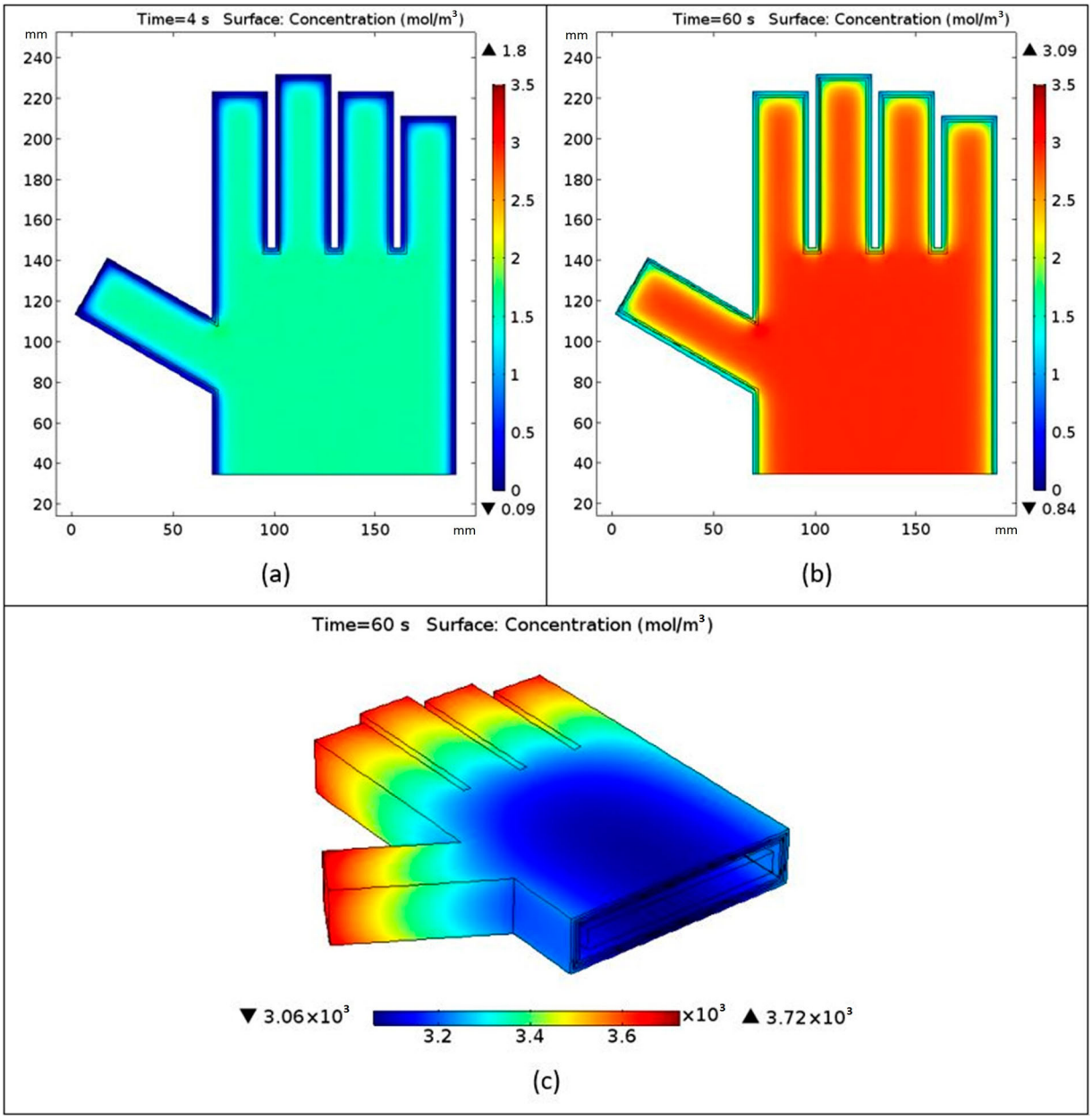

Figure 12. 3D vision of moisture concentration distribution in conventional firefighters' gloves (with no PCM). View at the cut plane of the interface between the base layer (inner thermal lining) and thermal barrier after (a) 4-s fire exposure and (b) 60-s air cooling period. (c) 3D view of the entire glove after a 60-s water cooling period. Note: 3D = three-dimensional; PCM = phase change material.

effects of pores in the skin. Hence, the heat transfer predictions in skin were reasonable. For the moisture transfer simulation, the main focus was on the water vapor transport in glove. We were not studying the moisture transfer in hand skin. Thus, the non-porous assumption for the hand skin would not affect the overall moisture transport phenomena in the glove. The hand sweating rate applied at the surface of the epidermis was based on the maximum skin sweating rate of the human body. The actual hand sweating rate may change based on different situations. Moreover, a fixed water spray rate was assumed at the glove's outer surface in the model. The actual water spray rate from an external hose may also vary in different situations. Thus, the absolute values from the simulation results may be different from actual situations, but the comparisons and trends of the results should be the same as those from the actual situations. Therefore, the numerical simulations can provide valuable information for the design of PCM-integrated structural firefighters' gloves in the future.

4.2. Validation

Experimental measurements have been conducted to verify the numerical simulation model [36]. The studies were conducted in a furnace environment under hazardous (furnace temperature of 200 °C with 10 kW/m^2 radiation heat flux) and lower bound of flashover (furnace temperature of 300 °C with 15 kW/m^2 radiation heat flux) conditions [36]. To better observe the PCM behavior and ensure safety, the testing environmental temperatures were not set at upper bound of flashover conditions. A commercial structural firefighting glove was used and cut into a 100 mm × 100 mm glove sample for testing. A PCM layer 1 mm thick (commercial bio-based PCM with a melting point of 68 °C) was inserted ABL in the glove sample. The glove sample materials along with the embedded PCM layer were attached on an insulation block to mimic a gloved hand (hand protected by glove), as shown in Figure 13. The temperatures on the insulation block surface were measured by three

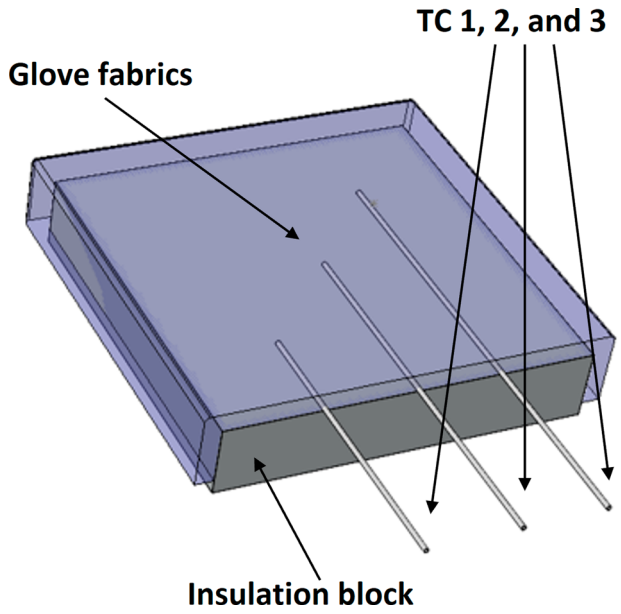

Figure 13. Glove sample materials along with the embedded PCM layer adhered/mounted on an insulation block to mimic a gloved hand [36]. Note: PCM = phase change material; TC = thermocouple.

thermocouples (TCs), representing the hand skin surface temperatures.

The numerical simulations were compared to the testing results under the same heat flux condition and PCM-integrated glove configuration, i.e., a bio-based PCM layer 1 mm thick (with melting point around 70 °C) located ABL in the glove. Figure 14 shows the temperature profiles on the hand skin surface from both numerical simulation and experimental testing. The temperatures at Probe 5 (numerical results; refer to Figure 3(a)) and temperatures at TC 2 (experimental results) were used for the comparison in Figure 14, because they all represented the center of the palm. The results were consistent with each other. The differences in temperature profiles between simulation and experiment were less than 15%. It was noted that better agreement between numerical and experimental studies occurred under higher heat flux condition. The experimental results showed that the optimum PCM melting temperature range was around 70–100 °C, the PCM location was better toward the environment in a glove under hazardous conditions and, overall, the PCM could extend the thermal protection time of firefighters' gloves (the time for hand skin to reach second degree burn injury) by 1.5–2 times [36], which is consistent with the numerical simulation results in this study.

5. Conclusion

As demonstrated in this study, the use of PCM could help remarkably improve the thermal protective performance of firefighters' gloves. Considering the hand dexterity and permeability of the glove, PCM was broken into several segments to be embedded in the glove's palm, back and finger areas, but avoiding all the finger joint areas. This study found that the PCM segments could extend the time for the hand skin surface to reach second-degree burn injury by more than two times compared to a conventional glove with no PCM. Furthermore, even for the areas not covered by PCM (such as joints), the PCM segments could still protect them to extend the time to reach second-degree burn injury by around 1.5 times.

The parametric study found that the PCM with a melting temperature range of 70–100 °C provided the best thermal protective performance for hand skin. The location of PCM segments depends on the condition of the fire scene. PCM provides better thermal protective performance when located close to the hand in the glove under flashover conditions. Further, PCM offers better thermal protection when located close to the environment in a glove under hazardous conditions.

A thicker PCM layer in the glove could provide better thermal protection for firefighters' hands. With PCM segments only 0.5 mm thick, the glove thermal protection time could be extended by up to a half-minute (around 30 s) compared to conventional firefighters' gloves (with no PCM) under hazardous conditions. When the thickness of PCM segments increases to 1 mm, the glove thermal protection time could be extended by more than 1 min under hazardous conditions (compared to the glove with no PCM). Nevertheless, the PCM

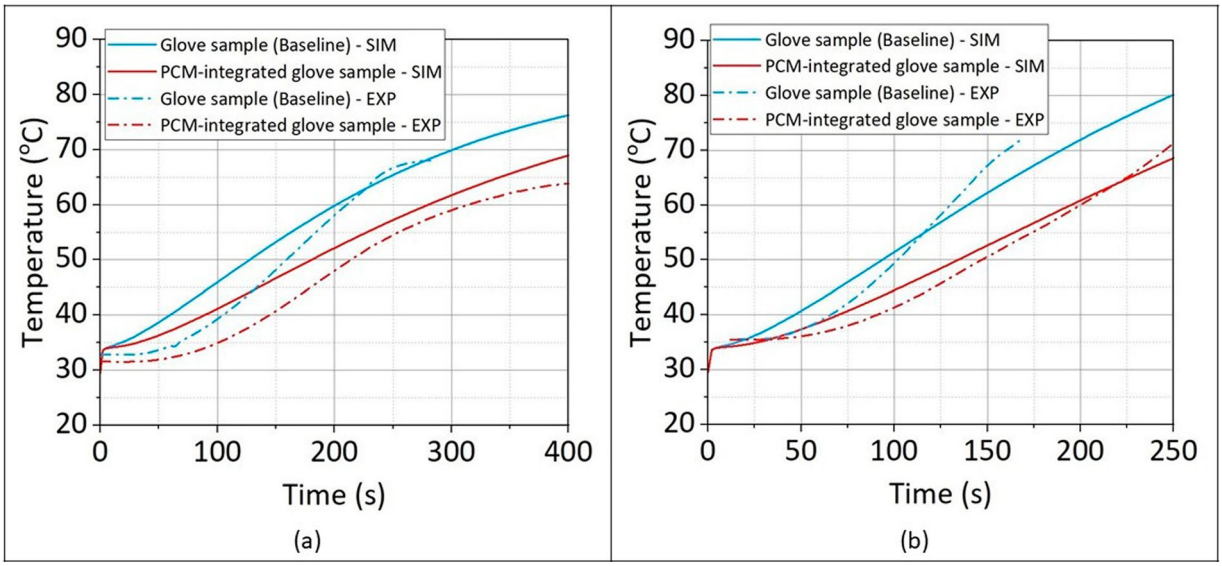

Figure 14. Comparison of temperatures on the hand surface between numerical simulation and experimental testing: (a) under hazardous condition (furnace temperature of 200 °C with 10 kW/m^2 radiation heat flux); (b) under lower bound of flashover condition (furnace temperature of 300 °C with 15 kW/m^2 radiation heat flux). Note: EXP = experimental testing results (TC 2); SIM = numerical simulation results (Probe 5); TC = thermocouple.

layer could not be too thick to compromise hand function. It requires a trade-off between hand thermal protection and dexterity. Thus, the optimum PCM thickness needs to be further explored considering both glove thermal protection and hand dexterity aspects in the future.

Moreover, PCM segments could block the moisture transfer to some degree and cause accumulation of moisture in some regions of the glove (such as at the PCM segment surface). Thus, the PCM segments' integration reduced the glove's overall moisture dissipation rate. However, the moisture could still move through the area not covered by PCM segments, maintaining the permeability of firefighters' gloves.

Disclaimer

The findings and conclusions in this report are those of the authors and do not necessarily represent the official position of the National Institute for Occupational Safety and Health, Centers for Disease Control and Prevention (NIOSH, CDC). Mention of any company or product does not constitute endorsement by the NIOSH, CDC.

Disclosure statement

No potential conflict of interest was reported by the authors.

Funding

This work was supported by Centers for Disease Control and Prevention National Institute for Occupational Safety and Health (CDC NIOSH) Nanotechnology Research Center (NTRC); CDC NIOSH Nanotechnology Research Center.

ORCID

Susan S. Xu http://orcid.org/0000-0003-4711-8658
Jonisha Pollard http://orcid.org/0000-0001-9282-9120
Weihuan Zhao http://orcid.org/0000-0001-9427-1001

References

[1] Coletta GC, Arons IJ, Ashley LE, et al. The development of criteria for firefighters' gloves volume II: glove criteria and test methods; NIOSH, Washington D.C.,1976 Feb. (Contract no. CDC-99-74-59.).
[2] U.S. Department of Homeland Security, Structural Firefighting Gloves Market Survey Report. System Assessment and Validation for Emergency Responders (SAVER), Washington, DC, October 2014.
[3] NFPA 1971 Standard on protective ensembles for structural fire fighting and proximity fire fighting; 2018.
[4] Campbell R, Hall S. United States firefighter injuries in 2021, NFPA Research [Internet]; November 30, 2023. Available from: https://www.nfpa.org/-/media/Files/News-and-Research/Fire-statistics-and-reports/Emergency-responders/osffinjuries.pdf
[5] Pro-Tech. A comprehensive guide on different firefighter gloves [Internet]. Available from: https://www.protech8.com/a-comprehensive-guide-on-different-types-of-firefighter-gloves/, November 12, 2024.
[6] US Department of Homeland Security, Science and Technology. Firefighter improved structure gloves receive NFPA certification, are available for use [Internet]; May 4, 2015. Available from: https://www.dhs.gov/science-and-technology/firefighter-glove-nfpa-certified
[7] NanoSonic. HybridShield thermal arrays [Internet]. Available from: https://nanosonic.com/products/hybridshield-thermal-arrays?_pos = 1&_sid = 5e9bb6385&_ss = r, November 12, 2024
[8] Gashti MP, Alimohammadi F, Song G, et al. Characterization of nanocomposite coatings on textiles: a brief review on microscopic technology. In: Méndez-Vilas A, editor. Current microscopy contributions to advances in science and technology, Microscopy Book Series Vol. 5. Chapter: Applications in Physical/Chemical Sciences. Norristown, PA: Formatex Research Centre; 2012. p. 1424–1437.
[9] Mondal S. Phase change materials for smart textiles – an overview. Appl Therm Eng. 2008;28:1536–1550. doi:10.1016/j.applthermaleng.2007.08.009
[10] Iqbal K, Khan A, Sun D, et al. Phase change materials, their synthesis and application in textiles – a review. The Journal of The Textile Institute. 2019;110(4):625–638. doi:10.1080/00405000.2018.1548088
[11] Pause B. Nonwoven protective garments with thermo-regulating properties. J Ind Text. 2003;33(2):93–99. doi:10.1177/1528083038859
[12] Lu Y, Wei F, Lai D, et al. A novel personal cooling system (PCS) incorporated with phase change materials (PCMs) and ventilation fans: an investigation on its cooling efficiency. J Therm Biol. 2015;52:137–146. doi:10.1016/j.jtherbio.2015.07.002
[13] Rossi RM, Bolli WP. Phase change materials for the improvement of heat protection. Adv Eng Mater. 2005;7(5):368–373. doi:10.1002/adem.200500064
[14] McCarthy LK, di Marzo M. The application of phase change material in fire fighter protective clothing. Fire Technol. 2012;48:841–864. doi:10.1007/s10694-011-0248-3
[15] Zhu F, Feng Q, Liu R, et al. Enhancing the thermal protective performance of firefighters' protective fabrics by incorporating phase change materials. Fibres Textiles Eastern Europe. 2015; 23:68–73.
[16] Barowy A, Madrzykowski D. The thermal behavior of structural firefighting protective ensemble samples modified with phase change material and exposed in full-scale room fires; Gaithersburg, MD, 2012. (NIST Technical Note 1739.).
[17] Hu Y, Huang D, Qi Z, et al. Modeling thermal insulation of firefighting protective clothing embedded with phase change material. Heat Mass Transfer. 2013;49:567–573. doi:10.1007/s00231-012-1103-x
[18] Fonseca A, Mayor TS, Campos JBLM. Guidelines for the specification of a PCM layer in firefighting protective clothing ensembles. Appl Therm Eng. 2018;133:81–96. doi:10.1016/j.applthermaleng.2018.01.028
[19] Fonseca A, Neves SF, Campos JBLM. Thermal performance of a PCM firefighting suit considering transient periods of fire exposure, post – fire exposure and resting phases. Appl Therm Eng. 2021;182:115769. doi:10.1016/j.applthermaleng.2020.115769
[20] Zhang H, Liu X, Song G, et al. Effects of microencapsulated phase change materials on the thermal behavior of multilayer thermal protective clothing. J Textile Inst. 2021;112(6):1004–1013. doi:10.1080/00405000.2020.1832363
[21] Xu SS, Pollard J, Zhao W. Modeling and analyzing for thermal protection of firefighters' glove by phase change material. J Environ Occup Health. 2022;12(2):118–127.
[22] PureTemp LLC. Global authority on phase change material [Internet]. Available from: https://puretemp.com/, November 12, 2024
[23] Su Y, Li R, Yang J, et al. Effect of compression on contact heat transfer in thermal protective clothing under different moisture contents. Cloth Text Res J. 2020;38(1):19–31. doi:10.1177/0887302X19863104
[24] Song G, Cao W, Gholamreza F. Analyzing stored thermal energy and thermal protective performance of clothing. Text Res J. 2011;81(11):1124–1138. doi:10.1177/0040517511398943
[25] Zhao W, France DM, Yu W, et al. Phase change material with graphite foam for applications in high-temperature latent heat storage systems of concentrated solar power plants. Renewable Energy. 2014;69:134–146. doi:10.1016/j.renene.2014.03.031
[26] Nawaz N, Troynikov O, Watson C. Evaluation of surface characteristics of fabrics suitable for skin layer of firefighters' protective clothing. Phys Procedia. 2011;22:478–486. doi:10.1016/j.phpro.2011.11.074
[27] Chae Y. Color appearance shifts depending on surface roughness, illuminants, and physical colors. Sci Rep. 2022;12:1371. doi:10.1038/s41598-022-05409-2
[28] Song G, Chitrphiromsri P, Ding D. Numerical simulations of heat and moisture transport in thermal protective clothing under flash fire conditions. Int J Occup Saf Ergon. 2008;14(1):89–106. doi:10.1080/10803548.2008.11076752
[29] Ventura G, Martelli V. Thermal conductivity of Kevlar 49 between 7 and 290 K. Cryogenics (Guildf). 2009;49:735–737. doi:10.1016/j.cryogenics.2009.08.001
[30] Ding D, Tang T, Song G, et al. Characterizing the performance of a single-layer fabric system through a heat and mass transfer model – part I: heat and mass transfer model. Text Res J. 2011;81(4):398–411. doi:10.1177/0040517510388547
[31] Incropera FP, DeWitt DP. Fundamentals of heat and mass transfer. 5th ed. Hoboken, NJ: Wiley; 2002.

[32] Harris JP, Yates B, Batchelor J, et al. The thermal conductivity of Kevlar fibre-reinforced composites. J Mater Sci. 1982;17:2925–2931. doi:10.1007/BF00644671
[33] Jessen C. Temperature regulation in humans and other mammals. Berlin: Springer; 2000.
[34] Sawka ML, Wenger CB, Pandolf KB. Chapter 9: Thermoregulatory responses to acute exercise-heat stress and heat acclimation. In: Fregly MJ, Blatteis CM, editors. Handbook of physiology. Section 4: environmental physiology. New York (NY): Oxford University Press; 1996. p. 157–185.
[35] Mack GW, Nadel ER. Chapter 10: Body fluid balance during heat stress in humans. In: Fregly MJ, Blatteis CM, editors. Handbook of physiology. Section 4: environmental physiology. New York (NY): Oxford University Press; 1996. p. 187–214.
[36] Wang X, Zhao W, Pollard J, et al. Experimental study on the thermal protection enhancement of novel phase change material integrated structural firefighting gloves under high-heat exposures. Case Stud Therm Eng. 2024;56:104286. doi: 10.1016/j.csite.2024.104286
[37] MetWeb (Material Property Data). Overview of materials for polytetrafluoroethylene (PTFE), extruded [Internet]. Available from: http://www.matweb.com/search/DataSheet.aspx?MatGUID = 4e0b2e88eeba4aaeb18e8820f1444cdb, November 12, 2024.
[38] MetWeb (Material Property Data). Overview of materials for polytetrafluoroethylene (PTFE), molded [Internet]. Available from: http://www.matweb.com/search/DataSheet.aspx?MatGUID = 4d14eac958e5401a8fd152e1261b6843&ckck = 1, November 12, 2024.